

Quantitative Image Analysis of Drug-Induced Lung Fibrosis Using Laser Scanning Confocal Microscopy

Michael D. Taylor,*† Jenny R. Roberts,† Ann F. Hubbs,† Mark J. Reasor,* and James M. Antonini†¹

*Department of Pharmacology and Toxicology, Robert C. Byrd Health Sciences Center of West Virginia University, Morgantown, West Virginia 26506;

†Health Effects Laboratory Division, National Institute for Occupational Safety and Health, 1095 Willowdale Road, Morgantown, West Virginia 26505

Received December 3, 2001; accepted January 30, 2002

Pulmonary fibrosis is a serious lung disorder that in certain cases may be difficult to quantify. It was our objective to evaluate the use of laser scanning confocal microscopy (LSCM) in quantifying fibrosis after exposure to amiodarone (AD) and bleomycin (BLM), two commonly used therapeutic drugs known to cause debilitating lung fibrosis in humans. Male F344 rats were intratracheally dosed with AD (6.25 mg/kg on days 0 and 2), BLM (0.25 and 1.0 mg/kg on day 0), or their respective vehicle controls. The right lung was assayed for hydroxyproline, a biochemical measure of collagen, at day 21 for the BLM groups and day 28 for the AD groups. The left lung was fixed, sectioned into blocks, dehydrated, stained with Lucifer yellow (LY, 0.1 mg/ml), and embedded in Spurr resin. The area of lung tissue stained by LY was quantified by LSCM. A fibrotic response in the AD and BLM groups was confirmed by histopathological assessment and a significant increase ($p < 0.05$) in total right lung hydroxyproline above control values. The area of connective tissue stained by LY of the two drug-treated groups appeared as bright linear bands in the alveolar septae and was significantly increased ($p < 0.05$) as measured by image analysis when compared with their respective controls. LSCM, with its advanced image analysis system, is an alternate method to quantify fibrotic lung disease. LSCM could be particularly useful when tissue quantity is limited, such as when tissue has been archived from previous studies, or when analyzing human lung biopsy samples for disease diagnosis, where biochemical analysis is difficult.

Key Words: amiodarone; bleomycin; fibrosis; laser scanning confocal microscopy; Lucifer yellow; three-dimensional reconstruction.

In conventional light microscopy, the whole depth of the specimen to be examined is uniformly and simultaneously illuminated (Wright *et al.*, 1993). This leads to out-of-focus light from areas above and below the focal plane of interest, thus reducing contrast and decreasing resolution. Moreover, when the light is directed below the specimen's surface, it becomes scattered, making it impossible to distinguish the object of interest and its surrounding environment. Laser scanning confocal microscopy (LSCM) offers many advantages

over conventional light microscopic techniques (Paddock, 1999). LSCM optics record only at the point of focus, removing flare and rejecting out-of-focus light from underlying and overlying structures of a sample (Inoue, 1989; Wright *et al.*, 1993). Rejection of out-of-focus light allows optical sectioning of the sample without physical disruption of the specimen, permitting large areas of the sample to be studied without sacrificing resolution. Series of optical sections taken at successive focal planes can then be stacked together to produce three-dimensional reconstructed views of the specimen. The image analysis systems integrated with most LSCMs provide rapid image formation and digital image collection for morphometric analysis, making LSCM a potentially powerful tool for quantitative studies (Smith *et al.*, 1991).

Pulmonary fibrosis is a chronic and incurable clinical condition that leads to a progressive accumulation of interstitial connective tissue (Witschi *et al.*, 1985). Interstitial pulmonary fibrosis is caused by an overaggressive repair process, which is accompanied by the presence of a large number of fibroblasts, an increase in absolute collagen levels, a thickening of the basement membrane, and an abnormal ultrastructural appearance. The most common way to quantify pulmonary fibrosis is to estimate collagen content by measuring lung hydroxyproline levels. This biochemical procedure is time consuming and labor intensive, destroys the lung specimen by digestion, and requires entire lungs for accurate analysis (Witschi *et al.*, 1985). Histopathology is also needed to distinguish the location and areas of fibrotic lesions. In previous studies, we have introduced the use of LSCM as a new method to quantify silica-induced pulmonary fibrosis (Antonini *et al.*, 1999).

It was the goal of this investigation to determine whether LSCM could be used as a potential diagnostic tool in assessing drug-induced lung fibrosis. Male Fischer 344 rats were dosed intratracheally with two therapeutically important agents, amiodarone (AD) and bleomycin (BLM). AD is a very effective antiarrhythmic drug that induces life-threatening pulmonary fibrosis in some patients (Mason, 1987). BLM is an antineoplastic agent that is highly effective in the treatment of some types of cancers, but produces a dose-dependent pulmonary fibrosis in most patients (Crystal *et al.*, 1976; Hesterberg *et al.*,

¹ To whom correspondence should be addressed. Fax: (304) 285-5938. E-mail: jga6@cdc.gov.

1981). Oftentimes diagnosis of debilitating pulmonary fibrosis is difficult in susceptible patients. Information collected by chest X-rays can be inconclusive. A new, reliable technique is needed to assess pulmonary fibrosis in both a quantitative and qualitative manner.

For this investigation, traditional methods of assessing lung fibrosis, such as histopathological analysis and lung weight and hydroxyproline measurements, were performed to establish that a fibrotic response had occurred after AD and BLM treatment. For analysis of drug-treated lungs with LSCM, the lungs were fixed, sectioned into blocks, dehydrated, stained with the fluorescent dye Lucifer yellow (LY), and embedded in Spurr plastic resin. Fluorescently labeled lung parenchyma was randomly scanned using LSCM, and the area of the connective tissue matrix within the alveolar walls stained by LY was measured. LY has been used in initial studies by our group and others to label the connective tissue of embedded lungs for LSCM imaging of the architecture of the lungs (Antonini *et al.*, 1996; Oldmixon and Carlsson, 1993; Rogers *et al.*, 1999).

MATERIALS AND METHODS

Materials

Amiodarone HCl was a gift from Wyeth-Ayerst Laboratories (Princeton, NJ). Bleomycin was purchased from Sigma Chemical Company (St. Louis, MO). Lucifer Yellow-CH was obtained from Molecular Probes (Eugene, OR). All other materials were laboratory grade and purchased commercially.

Laboratory Animals

All studies were performed on specific pathogen-free adult male F344 rats (200–300 g). Animals treated with AD or its control were purchased from Hilltop Laboratories (Scottsdale, PA), whereas animals treated with BLM or its control were obtained from Charles River Laboratories (Wilmington, MA). The animals were housed in the Robert C. Byrd Health Science Center's animal facility and were allowed at least one week to acclimate after arrival from supplier. Free access to food and water was allowed at all times.

Animal Treatment

Animals were anesthetized with 40 mg/kg Brevital (sodium methohexital; Eli Lilly Co., Indianapolis, IN), placed on a slanted board, and suspended from their maxillary incisors. The tongue was held with gauze, and a syringe with a ball-tipped 20-gauge feeding needle was inserted transorally into the trachea. AD (6.25 mg/kg in a 3.125 mg/ml solution) or the vehicle (sterile water) was administered in two intratracheal instillations, the first on what was designated day 0 and the second on day 2. BLM (0.25 mg/kg and 1.0 mg/kg) or the vehicle (sterile saline) was administered in one dose designated as day 0. Previous studies indicated that these dosing schedules produced pulmonary fibrosis using AD (Taylor *et al.*, 2000) and BLM (Ma *et al.*, 1999).

Analysis of Fibrosis

Animals were sacrificed with an overdose of sodium pentobarbital and exsanguinated by severing the abdominal aorta at day 21 for the BLM groups and day 28 for the AD group. After the trachea was cannulated, the right lung was ligated, removed, weighed, and frozen immediately at -70°C for later determination of hydroxyproline. The left lung was fully inflated and preserved with 10% buffered formalin by airway gravity fixation at a pressure of 30 cm water to ensure maximal lung inflation and eliminate any potential variability in inflation from animal to animal. Gil *et al.* (1979) demonstrated that when

inflating lung tissue with saline at a pressure of > 10 cm water, an inflation of $> 90\%$ of total lung capacity was reached.

Biochemical quantification of hydroxyproline. The frozen right lungs were thawed and minced, then processed and analyzed according to the method of Witschi *et al.* (1985). The chopped lungs were hydrolyzed in 6 N HCl at 100°C for 72 h, then neutralized with KOH. Aliquots of the hydrosylate were diluted in borate-alanine buffer and oxidized with chloramine T. The reaction was stopped with sodium thiosulfate, toluene was added, and the samples were boiled. After centrifugation, an aliquot of the organic phase was added to Ehrlich's reagent. Absorbance was read at 560 nm on a Gilford spectrophotometer. Trans-hydroxyproline was used as the standard for quantification.

Histopathological evaluation of fibrosis. Fibrosis was characterized histopathologically on fixed left lung tissue from sections that had been embedded in paraffin. Sections of $5\ \mu\text{m}$ were stained with either hematoxylin and eosin or trichrome, a stain that permits the identification of collagen fibers. Slides were then evaluated using light microscopy.

Confocal microscopy. Fixed left lung tissue was cut into blocks (~ 10 mm), dehydrated in a graded series of ethanol washes to absolute ethanol, fluorescently labeled with a 0.1 mg/ml concentration of Lucifer yellow for 24 h, washed in absolute ethanol, then embedded in Spurr's epoxy (Electron Microscopy Sciences, Fort Washington, PA) in preparation for analysis by confocal microscopy (Rogers *et al.*, 1999).

Images were recorded using a Sarastro 2000 laser scanning confocal microscope (Molecular Dynamics, Inc., Sunnyvale, CA) fitted with an argon-ion laser. Emission spectra > 510 nm were diverted to a separate photodetector and used to image lung tissue and cells. Using a $40\times$ objective, 25–50 random sections of lung parenchyma, excluding large airways, were scanned from each of four blocks of tissue for each animal. Three animals were used for analysis from each treatment group. Using ImageSpace software, the threshold pixel intensity levels that defined LY-positive and LY-negative sites were determined, and thus the presumed connective tissue matrix components were identified. To set the threshold, we interactively probed the images using a sliding gradient color map to effectively determine the intensity ranges of specific structures (0–20 pixel intensity units for air space, 21–79 pixel intensity units for air space cells and debris, > 80 pixel intensity units for connective tissue matrix components). Fluorescent signals below a pixel intensity value of 80, and thus below the threshold, were blocked, eliminating the measurement of cells and debris within the air spaces. All random scans of the lung tissue for each treatment group were recorded $\sim 3\text{--}5\ \mu\text{m}$ from the top of the tissue block at the same photo multiplier tube setting of 450–500, pinhole aperture setting of $50\ \mu\text{m}$, and at the same laser voltage setting of 20 mW. This analysis resulted in a data set expressed as connective tissue (LY-positive) area in μm^2 per image field. An image field $512\ \mu\text{m} \times 512\ \mu\text{m}$ ($2.62 \times 10^5\ \mu\text{m}^2$) was defined over a region of parenchyma entirely filling the field.

Randomly selected areas of embedded lung tissue from the different treatment groups were later scanned. Images of lung tissue from animals treated with BLM or its control were rendered from 75 serial optical sections, with $0.8\text{-}\mu\text{m}$ steps between each section. Three-dimensional projection series and stereo pairs were generated using ImageSpace, whereas three-dimensional reconstructions were created using Voxel View Ultra software (Vital Images, Inc., Fairfield, IA).

Statistical Analysis

Values for Table 1 and Figures 1 and 6 are expressed as means \pm standard error of measurement. Mean values for the treatment groups were compared using Student *t* test for nonpaired samples and by analysis of variance with Scheffe post hoc evaluation for the data set as a whole. Statistical analyses were performed using Statview statistical program (Abacus Concepts, Inc., Berkeley, CA). For all analyses, the criterion for significance was $p < 0.05$.

TABLE 1
Total Body and Right Lung Weights and Ratios

Treatment groups	Body weight (g)	Right lung weight (g)	Right lung/body weight ($\times 10^{-3}$)
Water control	277.0 \pm 4.5	0.702 \pm 0.016	2.54 \pm 0.07
AD	267.2 \pm 7.2	0.749 \pm 0.021	2.81 \pm 0.06*
Saline control	289.3 \pm 4.3	0.694 \pm 0.017	2.40 \pm 0.05
Low dose BLM	280.6 \pm 4.2	0.740 \pm 0.014	2.66 \pm 0.03*
High dose BLM	271.8 \pm 4.5	0.854 \pm 0.026*	3.14 \pm 0.07*†

Note. AD, amiodarone; BLM, bleomycin. $n =$ six rats per group.

* Indicates significantly greater than corresponding control.

† Indicates significantly greater than low dose BLM group ($p < 0.05$).

RESULTS

To confirm that intratracheal administration of AD and BLM induced pulmonary fibrosis, animal lung weights were determined, and hydroxyproline measurements and histopathology analyses were performed. Right lung weight/body weight ratio increased following AD and both BLM treatments, indicating a

possible fibrotic response (Table 1). Rats treated with AD and the high dose of BLM demonstrated significant elevations in right lung hydroxyproline values compared with their respective controls (Fig. 1). The hydroxyproline level for the low dose BLM group was no different from the control group (Fig. 1B). Histopathological evaluation of trichrome-stained left lung sections revealed a minimal to mild, multifocal, interstitial pulmonary fibrosis in all AD-treated rats. Fibrosis was most frequently observed near alveolar duct regions. High dose treatment with BLM induced a moderate, multifocal and coalescent, interstitial pulmonary fibrosis in treated rats, whereas low dose pulmonary administration of BLM caused a mild, multifocal, interstitial fibrosis (data not shown). Pulmonary fibrosis was not observed in any control animals. These results confirm that the intratracheal treatment models using AD and BLM are appropriate to further characterize pulmonary fibrosis using LSCM.

LY-stained lung tissue *en bloc* from each treatment group was examined with LSCM. Three-dimensional stereo projections (Fig. 2) and volume reconstructions (Fig. 3) of lung parenchyma 60 μm thick were rendered from saline control and high dose BLM-treated animals. Qualitative examination of LY-stained lung sections revealed connective tissue elements from both drug-treated and control animals. Abundant bands of lung connective tissue were clearly visible within the alveolar walls of the specimens, having a higher fluorescent intensity than lung cells such as macrophages and neutrophils within the alveolar spaces (Figs. 2A and 2B). A greater thickening of the alveolar septa was observed in the lung parenchyma of the drug-treated rats compared with controls. Focal accumulations of connective tissue elements were easily observed within the lungs of the drug-treated animals (Figs. 2B and 3B). The findings were very similar in the lungs of AD-treated rats (data not shown).

For quantification of the fibrotic response using LSCM, large volumes of LY-stained lung tissue from each treatment group were randomly scanned. In Figure 4, we show representative confocal micrographs in a pseudo-color intensity scale of a single optical section of lung parenchyma from the different groups. Lung tissue from control groups were normal (Figs. 4A and 4C). Intratracheal treatment with AD and high dose BLM

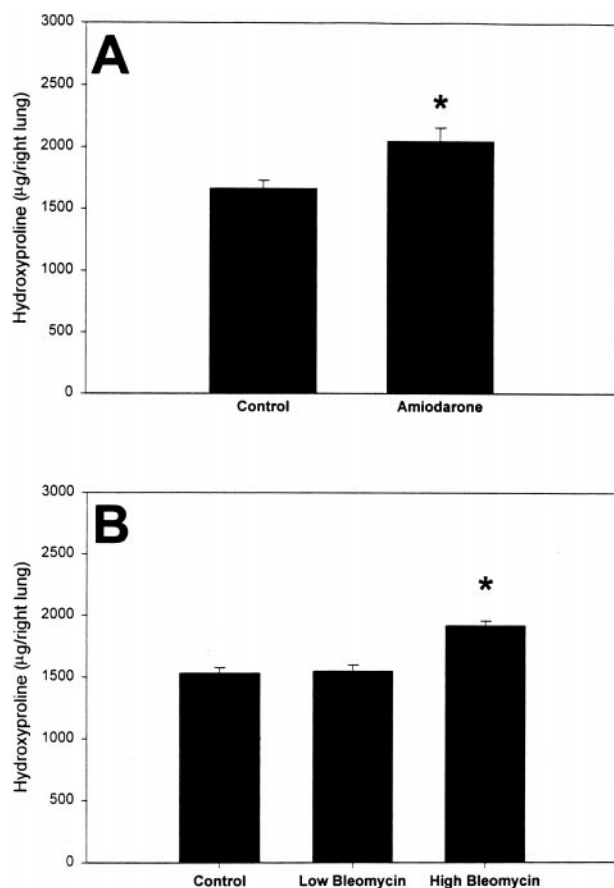


FIG. 1. Hydroxyproline content of right lungs after intratracheal administration: (A) amiodarone (6.25 mg/kg on days 0 and 2) and (B) bleomycin (low, 0.25 mg/kg, or high, 1.0 mg/kg, on day 0). *Indicates significantly greater than corresponding controls ($p < 0.05$); $n =$ six rats per group.

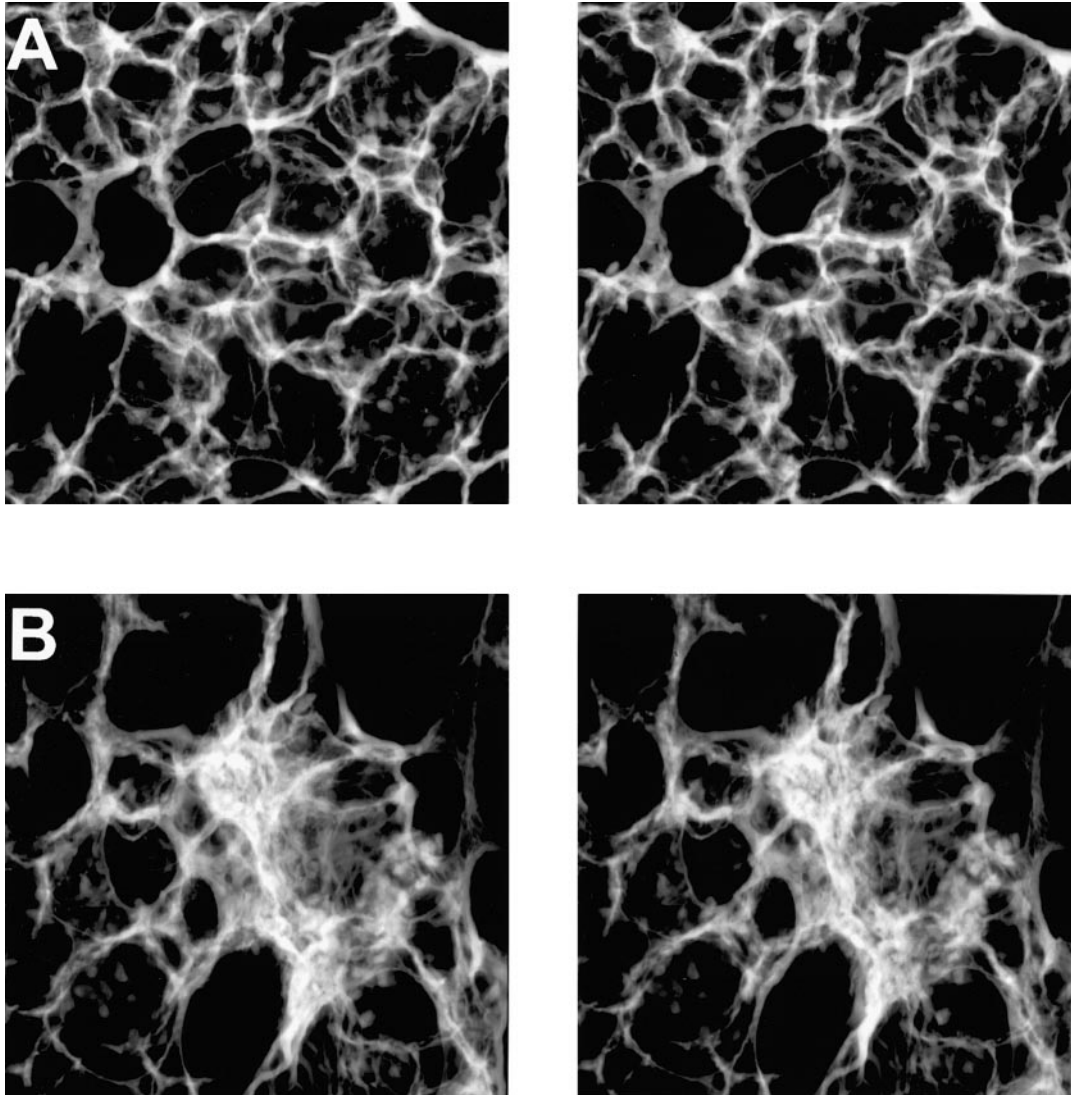


FIG. 2. Left and right panels of three-dimensional stereo projections of lung tissue stained with Lucifer yellow: (A) control and (B) high dose bleomycin (1.0 mg/kg on day 0). The three-dimensional images were rendered from 75 serial optical sections ($0.8 \mu\text{m}$ each) for a final thickness of $60 \mu\text{m}$ in depth. Eyeglass viewers will be supplied on request for reprints in order to observe the lung samples in three dimensions.

resulted in extensive tissue damage characterized by prominent focal thickening of alveolar walls, as illustrated by bright regions of fluorescence (Figs. 4B and 4D). The fluorescence within the image above a defined threshold was considered positive for LY staining and was summed to calculate the total connective tissue area in μm^2 per image area. Examples of confocal images of lung tissue with fluorescence above the defined threshold, used for quantification, are depicted in Figure 5. Background areas not quantified are displayed in gray, and LY-positive areas are displayed in green. Thus, cells and debris within the lung air spaces have been eliminated from the analysis of tissue area. AD caused a significant increase in LY-stained lung tissue area, as measured by LSCM compared with control (Fig. 6A). Interestingly, BLM caused a significant

dose-dependent increase in pulmonary fibrosis that was not observed in the analysis of lung hydroxyproline (Fig. 6B).

DISCUSSION

Pulmonary fibrosis is normally quantified by measuring the collagen content of lungs that have been dissolved in a strong acid or base. Hydroxyproline, an amino acid found exclusively in collagen, is measured by conventional biochemical methods (Haschek and Witschi, 1979; Witschi *et al.*, 1985). However, this approach can be tedious, requires fresh tissue, and destroys the specimen. The biochemical measurement of hydroxyproline is best applied to a defined anatomic lung unit (e.g., whole lung or lobe) for expression of the results. Because lung weight

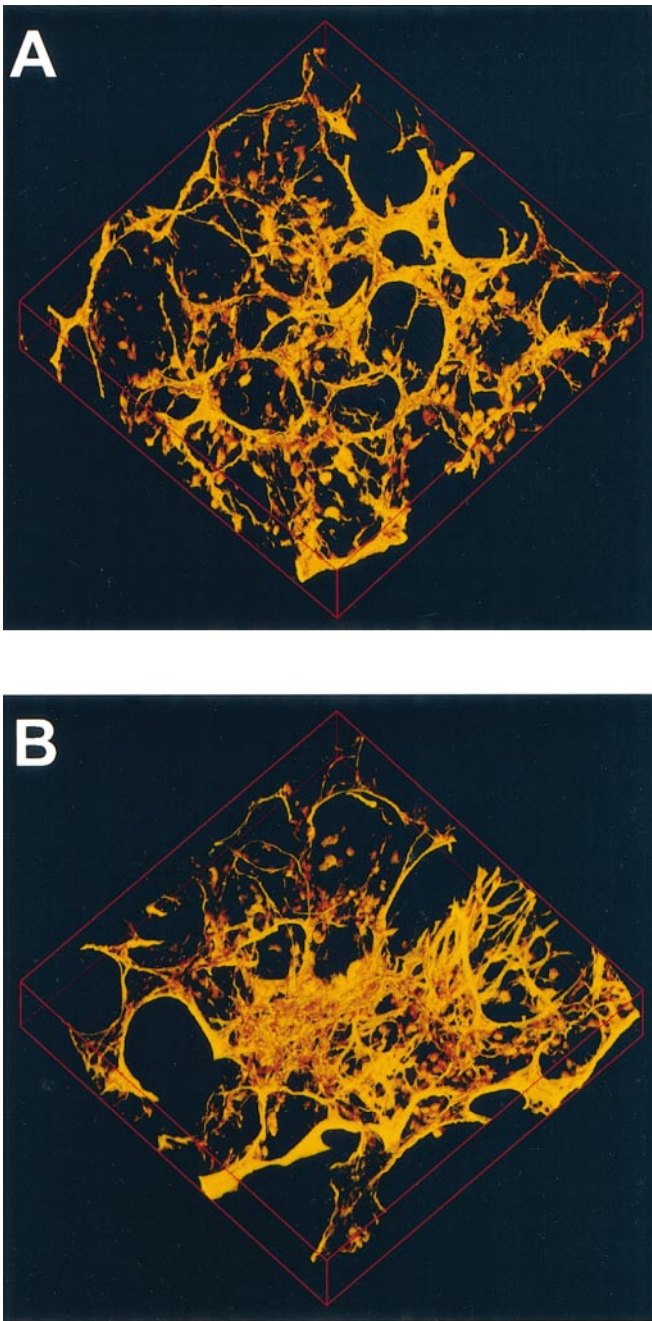


FIG. 3. Three-dimensional reconstruction of lung tissue stained with Lucifer yellow: (A) control and (B) high dose bleomycin (1.0 mg/kg on day 0). The three-dimensional images were rendered from 75 serial optical section steps (0.8 μm each) for a final thickness of 60 μm in depth.

increases with fibrosis and accompanying inflammation and edema are often present, expression of lung hydroxyproline per weight unit may underestimate the degree of collagen accumulation (Fulmer *et al.*, 1980; Witschi *et al.*, 1985). Histopathology is also needed to provide additional important information about the fibrotic response. Therefore, new image analysis methods are being developed to examine pulmonary fibrosis

both qualitatively and quantitatively in the same tissue specimen (Antonini *et al.*, 1999; Malkusch *et al.*, 1995).

Conventional light microscopy is a powerful tool to examine tissues and cells, but precise quantification of cellular responses is often difficult. Furthermore, it is useful only when generating images from very thin specimens. A major factor affecting the observation of thick tissue samples is that the specimens are significantly thicker than the depth-of-focus light of the microscope objective lens (Turner *et al.*, 2000). This results in loss of the contrast of in-focus image structure by out-of-focus light from specimen regions above and/or below the area of interest. If the specimen is sufficiently thick, the loss is so great that little or no in-focus structure is observed.

LSCM is providing new and exciting opportunities for imaging cell structures in thick biological specimens. The utility of LSCM relies on its fundamental capacity to reject out-of-focus light, thus providing sharp, high-contrast images of cells and subcellular structures in thick samples (Dailey *et al.*, 1999). With LSCM, sharp images are obtained by focusing the illuminating light on a single point in the plane of focus. Using stepper motors, the illuminating light is scanned across the plane of focus one point at a time, resulting in the elimination of light scatter. In addition, a pinhole aperture is placed in front of the light detector (the confocal point) that filters out all light emitted from structures above and/or below the plane of focus. Consequently, out-of-focus light is eliminated, resulting in an increase in contrast, clarity, and detection sensitivity (Inoue, 1989; Wright *et al.*, 1993). The resultant digital data, which encode the image, are highly amenable to processing, manipulation, and quantitation analyses (Turner *et al.*, 2000). Aided by the expansion in the number and specificity of fluorescent probes available, LSCM is being used in the development of advanced methodologies for the study of cell and tissue morphology.

In transmission electron microscopy (TEM), heavy metal stains are used to impart contrast to the tissues to be studied (Hayat, 1989). Rogers *et al.* (1992) attempted to determine whether the fluorescent stain LY was practical for LSCM studies with a correlative study using both TEM and LSCM. Using LSCM, they observed that fluorescent intensities of lung cells and connective tissue in 0.5- μm thick optical sections varied widely, depending on the structure labeled. When normalized from 0 to 1, fluorescent pixel intensities among corresponding structures in adjacent optical sections were consistent and repeatable with defined intensity ranges for elastin cables (0.84–1), collagen fibers (0.51–0.84), nucleoli (0.51–0.84), and nuclei (0.47–0.67). In other cellular structures, pixel intensity was variable among sections but had defined ranges for cell cytoplasm and interstitium (0.28–0.47), basement membrane (0.16–0.29), tissue surface/airspace interface (0.12–0.17), and epithelium and endothelium cytoplasm (0.02–0.06). Differences in form and pattern permitted distinction among cell types where pixel intensity overlapped. It was concluded that LY produces differential fluorescent staining of lung cells and connective tissue components comparable to the contrast of heavy metal-stained tissue sections in low-magnification TEM.

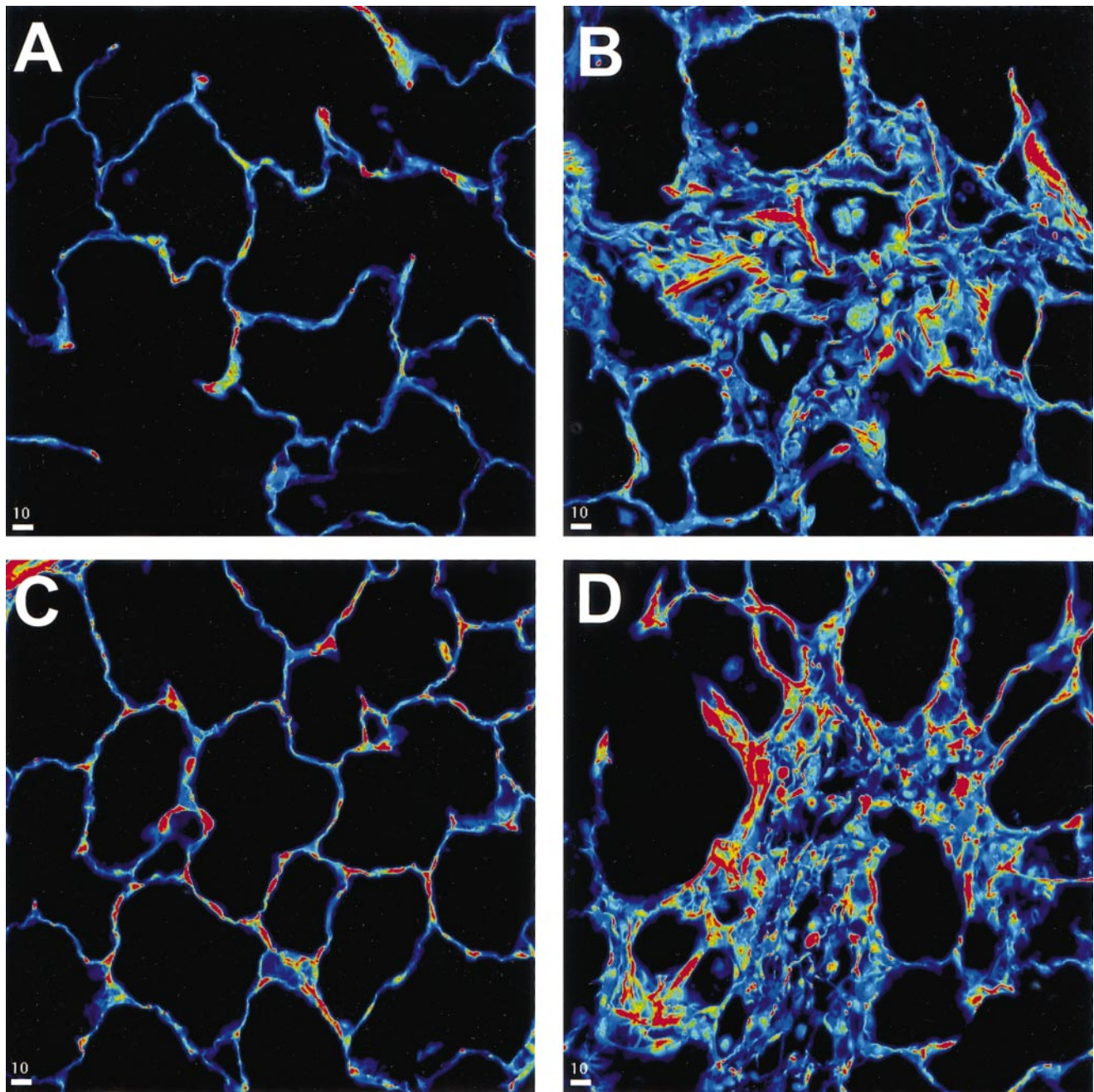


FIG. 4. Confocal micrographs of Lucifer yellow-stained lung tissue: (A) water control, (B) amiodarone (6.25 mg/kg on days 0 and 2), (C) saline control, and (D) high dose bleomycin (1.0 mg/kg on day 0). Lung tissue areas are depicted on a pseudo-color intensity scale. Low intensity sites are stained blue and higher intensity areas (connective tissue matrix) are stained green, yellow, red, and white, respectively, as intensity increased. Bar is 10 μ m.

Moreover, LY has been used in other LSCM investigations to study the deposition and clearance of occupational particles (Antonini *et al.*, 1996) and fibers (Rogers *et al.*, 1999), the lung anatomy and morphometry from large data volumes (Oldmixon and Carlsson, 1993), and the pulmonary fibrotic response to silica exposure (Antonini *et al.*, 1999; 2000).

It is of interest to note that BLM treatment caused a dose-dependent elevation in fibrosis as observed using LSCM.

When the lung tissue was analyzed by measuring hydroxyproline levels, the low dose BLM treatment did not demonstrate an increase in fibrosis, even though a fibrotic response was observed in lung sections stained with trichrome from the same animals of the low dose BLM group, and their right lung/body weight ratios were increased. These observations indicate that measuring the lung tissue area stained by LY using LSCM may be a more sensitive method to quantify pulmonary fibrosis

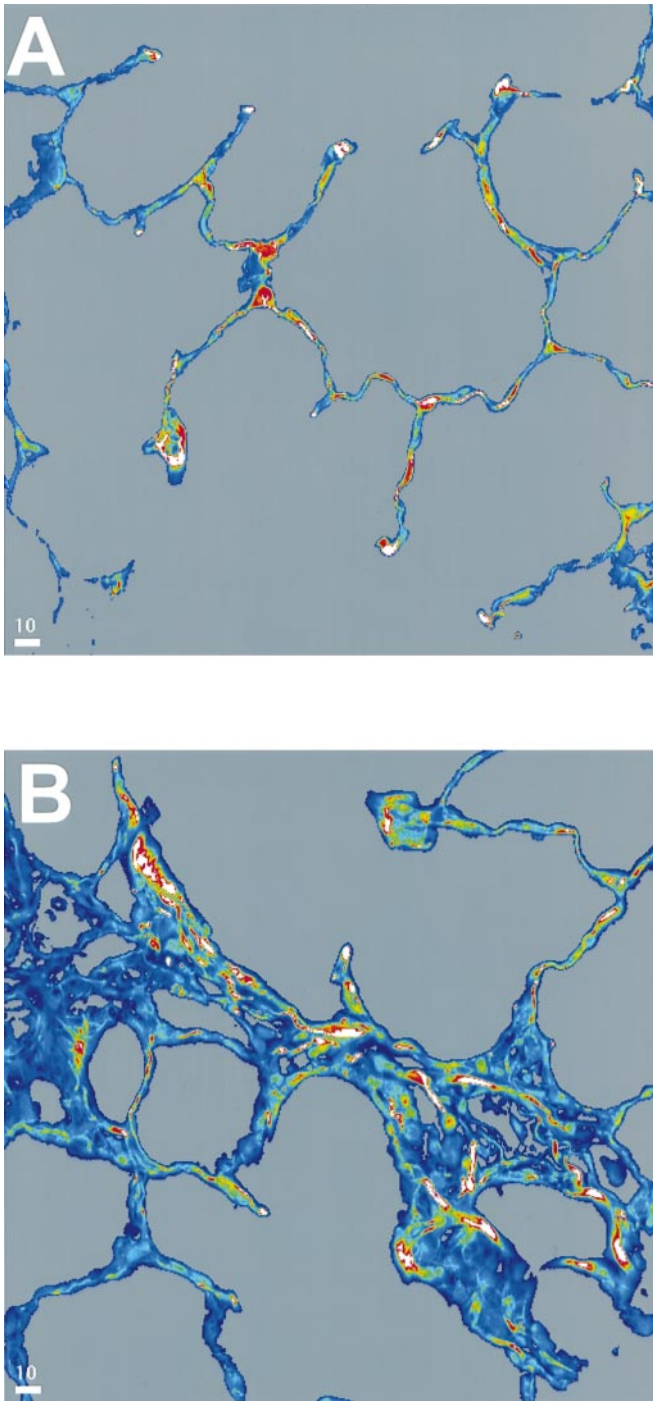


FIG. 5. Representative confocal images of lung tissue with fluorescence above the defined threshold, used for quantification: (A) control and (B) amiodarone (6.25 mg/kg on days 0 and 2). Background areas not quantified are displayed in gray. Bar is 10 μm .

compared with the biochemical method of determining hydroxyproline. This is not surprising, because the large airways could be specifically excluded from the tissue area measurements using LSCM, which is not the case when the entire lung sample needs to be digested for the determination of hy-

droxyproline. Using the fluorochrome Sirius Red, Malkusch *et al.* (1995) observed little change in the amount of collagen between groups that showed significant lesion formation compared with those that did not when entire lung samples were quantified by conventional light microscopy. However, when airway regions were excluded from the measurements, they observed a significant increase in lung collagen for the samples with fibrotic lesions, thus concluding that the increase was restricted to the alveolar regions of the lungs.

A distinct advantage in using LSCM to evaluate the extent of pulmonary fibrosis may come in the analysis of lung tissue samples that have been archived from previous studies. The fibrotic response in tissue sections from paraffin-embedded lung samples saved from a previously completed study (Davis *et al.*, 1998) that examined a model of silicosis in mice was evaluated by LY fluorescent dye staining and LSCM (Antonini *et al.*, 2000). It was observed that both LY image analysis and

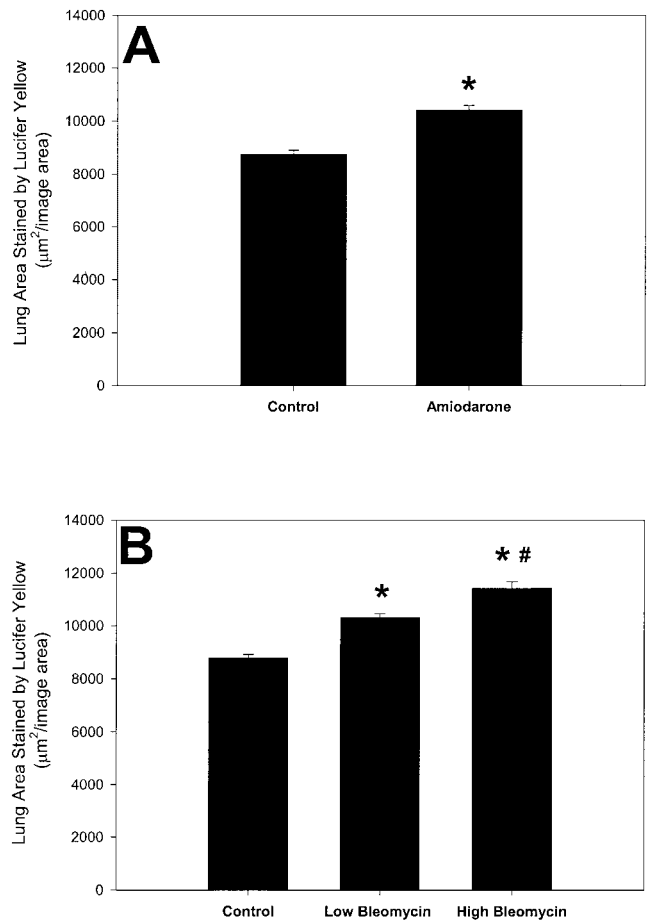


FIG. 6. Measured tissue area of Lucifer yellow-stained left lungs by confocal image analysis after intratracheal administration: (A) amiodarone (6.25 mg/kg on days 0 and 2) and (B) bleomycin (low, 0.25 mg/kg, or high, 1.0 mg/kg, on day 0). *Indicates significantly greater than corresponding controls; #Indicates significantly greater than low bleomycin group ($p < 0.05$); $n = 269$ lung sections for amiodarone and control groups in (A); $n = 299, 278,$ and 419 lung sections for high bleomycin, low bleomycin, and control groups, respectively, in (B).

biochemical hydroxyproline measurements demonstrated statistically significant differences based on mouse strain, exposure to silica, and time after exposure. For each group of mice, there was a statistically positive direct correlation between the amount of hydroxyproline measured and the lung tissue area stained by LY, illustrating that the measurements obtained by the LSCM method mirror the results of qualitative visual examination and biochemical quantification.

LSCM analysis may prove to be a powerful application for diagnostic purposes when using fresh or archived human lung biopsy samples where adequate amounts of tissue are not available for biochemical analysis or when an anatomic unit cannot be used for accurate expression of the results. For example, interest has evolved in evaluating lung samples that have been banked away for years in an attempt to determine the mechanisms of respiratory disease after the acute exposure to lethal smog levels in London during the winter of 1952 (Bell and Davis, 2001; Hunt *et al.*, 2001) or to chronic exposure to coal dust (Green *et al.*, 1998; Vallyathan *et al.*, 1996). LSCM analysis of archived lung tissue could then be especially useful in providing new insights in the study of environmental and workplace exposures to airborne hazards as well as assessing the lung disease status of individuals who are being treated with highly pneumotoxic drugs.

REFERENCES

- Antonini, J. M., Krishna Murthy, G. G., Rogers, R. A., Albert, R., Ulrich, G. D., and Brain, J. D. (1996). Pneumotoxicity and pulmonary clearance of different welding fumes after intratracheal instillation in the rat. *Toxicol. Appl. Pharmacol.* **140**, 188–199.
- Antonini, J. M., Charron, T. G., Roberts, J. R., Lai, J., Blake, T. L., and Rogers, R. A. (1999). Application of laser scanning confocal microscopy in the analysis of particle-induced pulmonary fibrosis. *Toxicol. Sci.* **51**, 126–134.
- Antonini, J. M., Hemenway, D. R., and Davis, G. S. (2000). Quantitative image analysis of lung connective tissue in murine silicosis. *Exp. Lung Res.* **26**, 71–88.
- Bell, M. L., and Davis, D. L. (2001). Reassessment of the lethal London fog of 1952: Novel indicators of acute and chronic consequences of acute exposure to air pollution. *Environ. Health Perspect.* **109**(Suppl. 3), 389–394.
- Crystal, R. G., Fulmer, J. D., Roberts, W. C., Moss, M. L., Line, B. R., and Reynolds, H. Y. (1976). Idiopathic pulmonary fibrosis. Clinical, histologic, radiographic, physiologic, scintigraphic, cytologic, and biochemical aspects. *Ann. Intern. Med.* **85**, 769–788.
- Dailey, M., Marrs, G., Satz, J., and Waite, M. (1999). Concepts in imaging and microscopy. Exploring biological structure and function with confocal microscopy. *Biol. Bull.* **197**, 115–122.
- Davis, G. S., Leslie, K. O., and Hemenway, D. R. (1998). Silicosis in mice: Effects of dose, time, and genetic strain. *J. Environ. Pathol. Toxicol. Oncol.* **17**, 81–97.
- Fulmer, J. D., Bienkowski, R. S., Cowan, M. J., Breul, S. D., Bradley, K. M., Ferrans, V. J., Roberts, W. C., and Crystal, R. G. (1980). Collagen concentration and rates of synthesis in idiopathic pulmonary fibrosis. *Am. Rev. Respir. Dis.* **122**, 289–301.
- Gil, J., Bachofen, H., Gehr, P., and Weibel, E. R. (1979). Alveolar volume-surface area relation in air- and saline-filled lungs fixed by vascular perfusion. *J. Appl. Physiol.* **47**, 990–1001.
- Green, F. H. Y., Althouse, R., Parker, J., Kahn, J., Weber, K., and Vallyathan, V. (1998). Trends in the prevalence of coal workers' pneumoconiosis in US autopsied coal miners. In *Advances in the Prevention of Occupational Respiratory Diseases* (K. Chiyotani, Y. Hosoda, and Y. Aizawa, Eds.), pp. 145–148. Elsevier Science, New York.
- Haschek, W. M., and Witschi, H. P. (1979). Pulmonary fibrosis—a possible mechanism. *Toxicol. Appl. Pharmacol.* **51**, 475–487.
- Hayat, M. A. (1989). Positive staining. In *Principles and Techniques of Electron Microscopy: Biological Applications* (M. A. Hayat, Ed.), 3rd ed., p. 318. CRC Press, Inc., Boca Raton, FL.
- Hesterberg, T. W., Gerriets, J. E., Reiser, K. M., Jackson, A. C., Cross, C. E., and Last, J. A. (1981). Bleomycin-induced pulmonary fibrosis: Correlation of biochemical, physiological, and histological changes. *Toxicol. Appl. Pharmacol.* **60**, 360–367.
- Hunt, A., Judson, B., Berry, C. L., and Abraham, J. L. (2001). Fine particulate metals inhaled at the time of the London Smog of 1952: Clues from lung tissue compartmental microanalysis. *Am. J. Respir. Crit. Care Med.* **163**, A175.
- Inoue, S. (1989). The principles of confocal microscopy. In *The Handbook of Biological Confocal Microscopy* (J. Pawley, Ed.), pp. 1–13. IMR Press, Madison, WI.
- Ma, J. Y. C., Barger, M. W., Hubbs, A. F., Castranova, V., Weber, S. L., and Ma, J. K. H. (1999). Use of tetrandrine to differentiate between mechanisms involved in silica- versus bleomycin-induced fibrosis. *J. Toxicol. Environ. Health A* **56**, 247–266.
- Malkusch, W., Rehn, B., and Bruch, J. (1995). Advantages of Sirius Red staining for quantitative morphometric collagen measurements in lungs. *Exp. Lung Res.* **21**, 67–77.
- Mason, J. W. (1987). Amiodarone. *N. Engl. J. Med.* **316**, 455–466.
- Oldmixon, E. H., and Carlsson, K. (1993). Methods for large data volumes from confocal scanning laser microscopy of lung. *J. Microsc.* **170**, 221–228.
- Paddock, S. W. (1999). Confocal laser scanning microscopy. *Biotechniques* **27**, 992–1004.
- Rogers, R. A., Oldmixon, E. H., and Brain, J. D. (1992). Enhanced contrast within embedded tissue by lucifer yellow CH: an ideal stain for laser scanning confocal microscopy. *Mol. Biol. Cell* **3**, 185a.
- Rogers, R. A., Antonini, J. M., Brismar, H., Lai, J., Hesterberg, T. W., Oldmixon, E. H., Thevenaz, P., and Brain, J. D. (1999). *In situ* microscopic analysis of asbestos and synthetic vitreous fibers retained in hamster lungs following inhalation. *Environ. Health Perspect.* **107**, 367–375.
- Smith, G. J., Bagnell, C. R., Bakewell, W. E., Black, K. A., Bouldin, T. W., Earnhardt, T. S., Hook, G. E. R., and Pryzwansky, K. B. (1991). Application of confocal scanning laser microscopy in experimental pathology. *J. Electron Microsc. Tech.* **18**, 38–49.
- Taylor, M. D., Van Dyke, K., Bowman, L. L., Miles, P. R., Hubbs, A. F., Mason, R. J., Shannon, K., and Reasor, M. J. (2000). A characterization of amiodarone-induced pulmonary toxicity in F344 rats and identification of surfactant protein-D as a potential biomarker for the development of the toxicity. *Toxicol. Appl. Pharmacol.* **167**, 182–190.
- Turner, J. N., Shain, W., Szarowski, D. H., Lasek, S., Dowell, N., Sipple, B., Can, A., Al-Kofahi, K., and Roysam, B. (2000). Three-dimensional light microscopy: Observation of thick objects. *J. Histotechnol.* **23**, 205–217.
- Vallyathan, V., Brower, P. S., Green, F. H. Y., and Attfield, M. D. (1996). Radiographic and pathologic correlation of coal workers' pneumoconiosis. *Am. J. Respir. Crit. Care Med.* **154**, 741–748.
- Witschi, H. P., Tryka, A. F., and Lindenschmidt, R. C. (1985). The many faces of an increase in lung collagen. *Fundam. Appl. Toxicol.* **5**, 240–250.
- Wright, S. J., Centonze, V. E., Stricker, S. A., DeVries, P. J., Paddock, S. W., and Schatten, G. (1993). Introduction to confocal microscopy and three-dimensional reconstruction. In *Methods in Cell Biology* (B. Matsumoto, Ed.), Vol. 38, pp. 1–45. Academic Press, New York.